

Epithelial cell shape is regulated by Lulu proteins via myosin-II

Hiroyuki Nakajima and Takuji Tanoue*

Global COE Program for Integrative Membrane Biology, Graduate School of Medicine, Kobe University, Chuo-ku, Kobe 650-0017, Japan

*Author for correspondence (tanoue@med.kobe-u.ac.jp)

Accepted 19 November 2009

Journal of Cell Science 123, 555–566

© 2010. Published by The Company of Biologists Ltd

doi:10.1242/jcs.057752

Summary

Cell-shape change in epithelial structures is fundamental to animal morphogenesis. Recent studies identified myosin-II as the major generator of driving forces for cell-shape changes during morphogenesis. Lulu (Epb4115) is a major regulator of morphogenesis, although the downstream molecular and cellular mechanisms remain obscure in mammals. In *Drosophila* and zebrafish, Lulu proteins were reported to negatively regulate Crumbs, an apical domain regulator, thus regulating morphogenesis. In this study, we show that mammalian Lulu activates myosin-II, thus regulating epithelial cell shape. In our experiments, Lulu expression in epithelial cells resulted in apical constriction and lateral elongation in the cells, accompanied by upregulation of myosin-II. The inhibition of myosin-II activity almost completely blocked this Lulu-driven cell-shape change. We further found that Rock participates in the myosin-II activation. Additionally, RNAi-mediated depletion of Lulu in epithelial cells resulted in disorganization of myosin-II and a concomitant loss of proper lateral domain organization in the cells. From these results, we propose that Lulu regulates epithelial cell shape by controlling myosin-II activity.

Key words: Epithelial organization, Cell shape, Apical constriction, Myosin-II

Introduction

The plasma membrane in polarized epithelial cells is divided into apical and basolateral domains, which differ in their protein and lipid compositions. The ratio of the sizes of these two distinct membrane domains changes according to the cell type and developmental stage. Apical constriction and lateral elongation in epithelial cells are thought to trigger invagination and the folding of epithelial cell sheets by changing individual cells from a cuboidal to bottle-like morphology (Lecuit and Lenne, 2007; Pilot and Lecuit, 2005). Apical constriction is mainly driven by the myosin-II–F-actin network positioned in the apical portion of the cells (Lecuit and Lenne, 2007; Lee and Harland, 2007; Martin et al., 2009). Myosin-II is activated by the phosphorylation of myosin regulatory light chains (MRLCs) mediated by several kinases, including Rho-associated kinase (Rock) (Matsumura and Hartshorne, 2008). Actually, Rock is thought to participate in apical constriction (Dawes-Hoang et al., 2005; Escudero et al., 2007; Hildebrand, 2005). Several regulators of apical constriction that activate the Rock–myosin-II axis have been well characterized in *Drosophila*. For example, the secreted molecule FOG (folded gastrulation) triggers apical constriction during mesoderm invagination by activating the Rock–myosin-II axis via the RhoGEF2–Rho–Rock pathway positioned in the apical portion (Barrett et al., 1997; Costa et al., 1994; Dawes-Hoang et al., 2005; Hacker and Perrimon, 1998; Kolsch et al., 2007). However, in vertebrates, Shroom3 is the sole identified candidate for regulating apical constriction upstream of the Rock–myosin-II axis (Haigo et al., 2003; Hildebrand, 2005; Hildebrand and Soriano, 1999; Nishimura and Takeichi, 2008). Thus, in vertebrates, the molecular mechanisms regulating cell-shape change during morphogenesis are not yet fully understood.

Recently, a FERM protein, Lulu (also known as Epb4115, erythrocyte protein band 4.1-like 5), was reported to regulate mammalian morphogenesis: Lulu mutant mice exhibited embryonic

lethality with defects in gastrulation and folding of the neural plate (Garcia-Garcia et al., 2005; Hirano et al., 2008; Lee, J. D. et al., 2007). In terms of mechanistic aspects, it was proposed that Lulu downregulates the E-cadherin level, and upregulates the integrin level, thus accelerating epithelial-mesenchymal transition. Lulu was shown to interact with p120 catenin and paxillin at cell-cell junctions and focal contacts, respectively (Hirano et al., 2008). In addition, Lulu (Epb4115) has one homologous molecule in mammals, Ehm2 (Epb4114b), although its function has not been fully elucidated (Chauhan et al., 2003; Shimizu et al., 2000). In this study, the homologs have been renamed Lulu1 and Lulu2, respectively. In zebrafish, Moe, the sole Lulu molecule in the species, is required for layering of the retina and inflation of the brain ventricles, as well as restricting the photoreceptor apical domain (Hsu et al., 2006; Jensen and Westerfield, 2004). It was shown that Moe interacts with and negatively regulates Crumbs, a regulator of the apical membrane domain, thus regulating the apical membrane size in epithelial structures (Hsu et al., 2006). Lulu also plays important roles in invertebrates: in *Drosophila*, mutant animals of Yurt, which is thought from sequence similarity to be an ortholog of Lulu, display failures in early epithelial morphogenesis, including head involution and germ-band elongation (Hoover and Bryant, 2002). At the cellular level, loss of Yurt causes an extension of the apical membrane of the cells, which is also proposed to be due to the misregulation of Crumbs (Laprise et al., 2006); however, our knowledge of the cellular and molecular functions of Lulu molecules, especially in mammals, is still limited.

In this study, we explored the molecular and cellular functions of mammalian Lulu1 and Lulu2 in polarized epithelial cells and found that they commonly have strong activities in terms of facilitating cell-shape change: their expression resulted in apical constriction and lateral elongation of polarized epithelial cells. The

cell-shape change induced by Lulu proteins is caused by the upregulation of myosin-II activity at the cell cortex, which is partially mediated by Rock. This upregulation is independent of Shroom3. Furthermore, we found that loss of Lulu proteins by RNAi in epithelial cells resulted in disorganization of myosin-II-F-actin networks, as well as the concomitant loss of proper lateral structures in the cells. We thus propose here that Lulu proteins commonly regulate epithelial cell shape by controlling myosin-II activity.

Results

Lulu proteins are mainly localized at the basolateral portion in polarized epithelial structures

Both Lulu1 and Lulu2 have two alternatively spliced transcripts that share FERM and FERM-adjacent (FA) domains in their N-terminal portions (Fig. 1A) (Baines, 2006; Lee, J. D. et al., 2007; Shimizu et al., 2000). The C-terminal portions of the isoforms do not have obvious homology among them. As the long form of Lulu1 (Lulu1-L) was the best characterized among them, we generated an antibody against Lulu1-L and mapped its protein distribution in mouse embryos (for the specificity of the antibody, see supplementary material Fig. S1). Analyses using this antibody revealed that Lulu1-L was widely distributed in several epithelial structures, including the kidney epithelium and neuroepithelium

(Fig. 1B,C). In these epithelial structures, Lulu1-L was mainly detected at the basolateral membranes, overlapping β -catenin, a basolateral membrane marker (Fig. 1C). Consistent with this observation, all isoforms of Lulu1 and Lulu2 were mainly detected in the basolateral portion of the cells when exogenously expressed in MDCK cells, although Lulu2 molecules exhibit cytoplasmic localization as well as basolateral membrane localization, and Lulu1 was more efficiently localized in lateral membranes than Lulu2 (Fig. 1D,E, and our unpublished data; see also other later figures showing Lulu localization). These results indicate that Lulu proteins are mainly basolateral molecules.

Lulu proteins induce apical constriction in epithelial cells

To explore the function of Lulu proteins in epithelial cells, we utilized MDCK cells, which have been widely used as a model system of polarized epithelial cells. First, we expressed Lulu proteins via a transient transfection method to obtain a small number of cells expressing Lulu1-L. In such cultures, Lulu-expressing cells exhibit apical constriction (Fig. 2A,B). There is a difference in the magnitude of this activity: Lulu2 molecules have more potent activity than Lulu1 molecules ($n>100$, $P<0.005$). A reduction of apical areas by Lulu expression was also observed by using other epithelial cells, including DLD1, NRK52E and Caco-2 cells, and

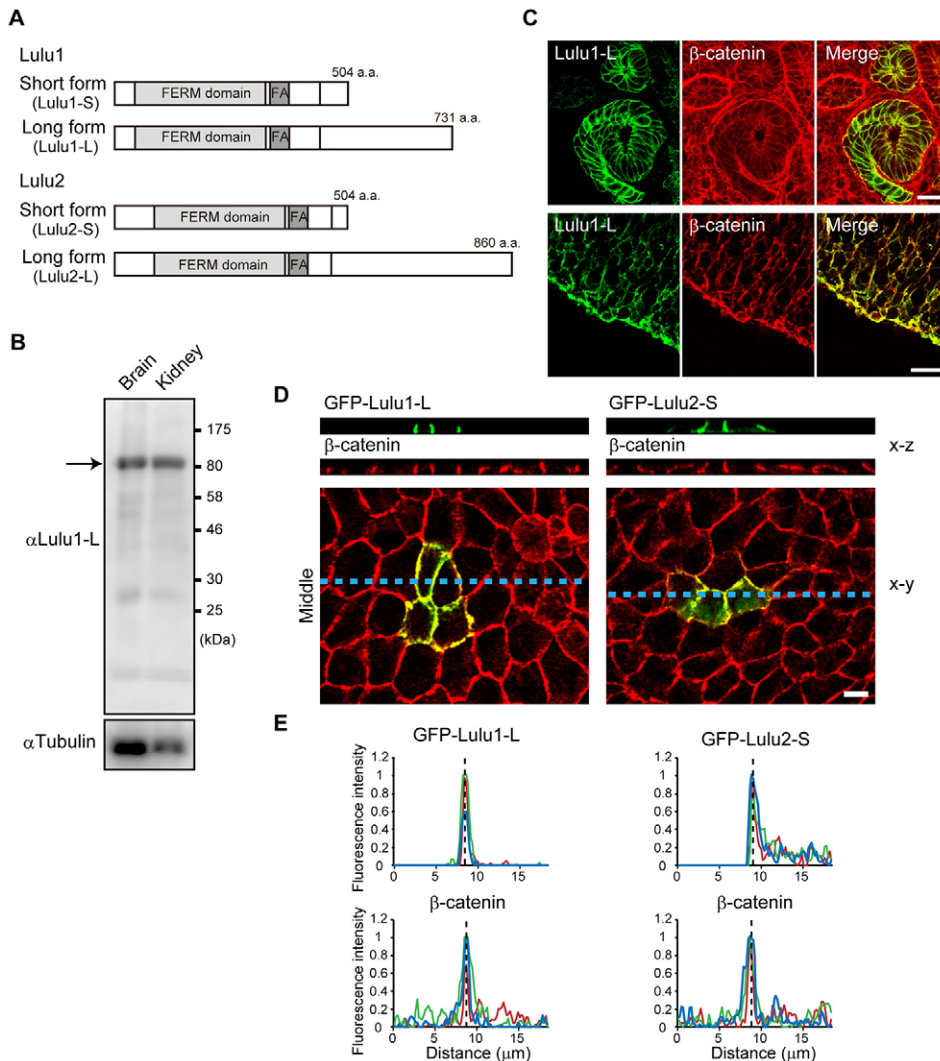


Fig. 1. Basolateral localization of Lulu proteins in polarized epithelial structures. (A) Mouse Lulu molecules showing FERM and FA domains. (B) Immunoblotting, to detect Lulu1-L in lysates of the brain or kidney of E12.5 mice. (C) E14.5 kidney (upper) and E14.5 cerebral cortex (lower) doubly immunostained for Lulu1-L and β -catenin. Lulu1-L overlaps β -catenin. (D) MDCK cells transfected with GFP-Lulu1-L or GFP-Lulu2-S doubly immunostained for GFP-Lulu and β -catenin. Middle confocal sections of cells are shown in lower panels. Images in upper panels are vertical sections of the portion indicated by blue dotted lines in lower panels (x-z). (E) Fluorescence intensity of GFP-Lulu or β -catenin signals scanned across cell-cell boundaries between control and Lulu-expressing cells (left and right of dotted lines, respectively). Three different cell-cell boundaries were measured (shown in different three colors). Lulu proteins overlap β -catenin. Scale bars: 20 μ m (C), 10 μ m (D).

this reduction indicates that Lulu-induced apical constriction is not a specific event in MDCK cells (our unpublished data). As the results obtained in this study are essentially the same among Lulu molecules, despite some differences in phenotypic strength, the results for Lulu1-L and the short form of Lulu2 (Lulu2-S) are presented as representatives. As epithelial cell-shape changes during morphogenesis usually take place in cell sheets, we prepared MDCK Tet-Off cells that can be induced to express myc-tagged Lulu molecules (Fig. 2C; supplementary material Fig. S2A) and then examined the phenotypes of the cells when mixed with parental cells. In these mixed-cell cultures, Lulu-expressing cells again exhibited reduced apical areas compared with their non-expressing neighbors (Fig. 2D,E; supplementary material Fig. S2B,C). This phenotype was stronger in Lulu2-expressing cells than in Lulu1-expressing cells (Fig. 2E), in good agreement with the results obtained in our transient transfection experiments (Fig. 2A,B). In addition, in these mixed-cell cultures, apical areas in non-expressing neighboring cells became enlarged (Fig. 2D,E), which is probably due to mechanical tensions generated by constricting Lulu-expressing cells.

Because the apical membrane size became reduced in Lulu-expressing cells, we next asked whether molecules regulating apical domain organization became mislocalized in Lulu-expressing cells. There are two major molecular complexes regulating apical domain organization: the Crumbs and Par complexes, both of which are localized along apical cell-cell boundaries and at apical membranes

(Wang and Margolis, 2007). By immunostaining Crb3 or Par3 (components of the Crumbs and Par complexes, respectively) we found that they were not downregulated, but upregulated, in the apical portion of Lulu2-S-expressing cells (supplementary material Fig. S2D). These results suggest that apical determinants are not negatively regulated by Lulu expression, although the apical membrane size became reduced by Lulu expression.

It was reported that Shroom3, another well-known regulator of apical constriction, upregulates apical tension and thereby strains apical cell-cell boundaries marked by ZO-1 (Zonula occludens protein 1) staining in MDCK cells (Hildebrand, 2009). To test whether Lulu proteins also enhance apical tension, we examined ZO-1 staining in Lulu-expressing cells without mixing with parental cells, and found that Lulu-expressing cells also exhibited more strained cell-cell boundaries than parental cells (supplementary material Fig. S2E). This result indicates that Lulu proteins also upregulate apical tension, and suggests that molecules with apical constricting activity commonly possess activity to enhance apical tension.

Both FERM and FA domains are necessary and sufficient to drive apical constriction

To identify the region responsible for apical constriction, we examined several deletion mutants of Lulu for their ability to drive apical constriction (Fig. 3A). We mainly examined Lulu2-S molecule for this activity, as it exhibits the most potent activity

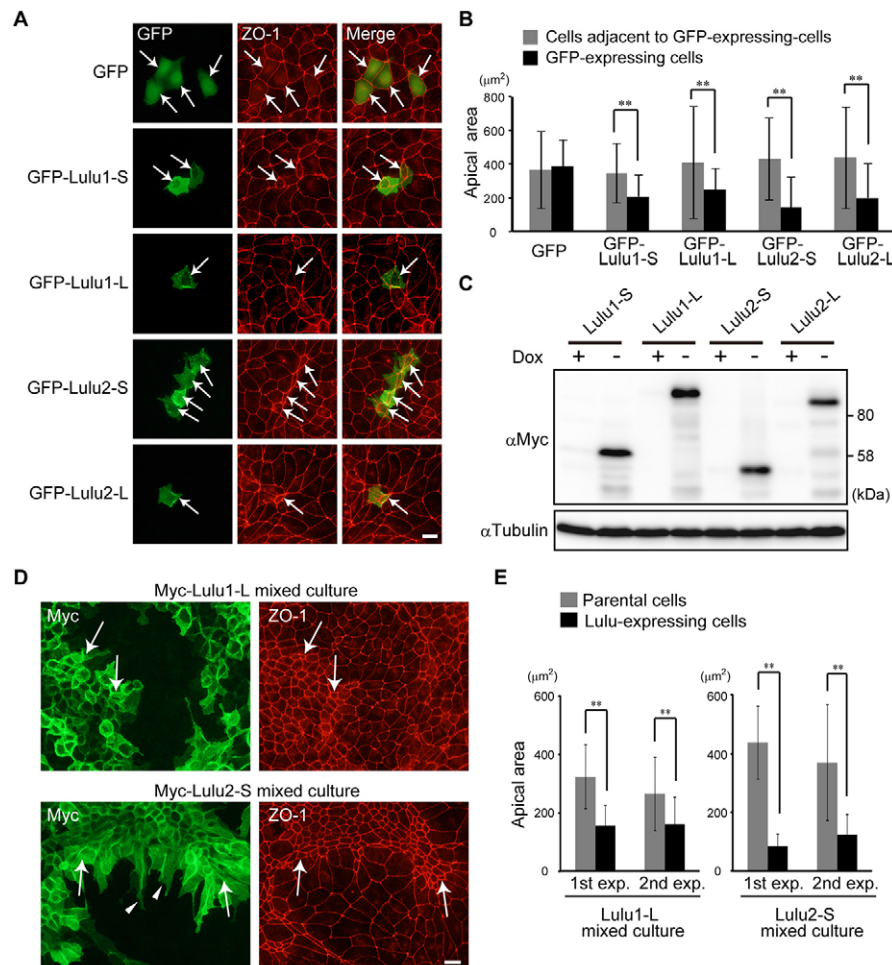


Fig. 2. Lulu proteins induce apical constriction.

(A) MDCK cells were transiently transfected with GFP or GFP-Lulu isoforms and subsequently doubly immunostained for GFP and ZO-1. All images were made by focusing ZO-1. Arrows indicate GFP-expressing cells. (B) Measurement of apical areas of GFP-expressing cells and cells adjacent to GFP-expressing cells shown in A. (C) MDCK Tet-Off cells inducibly expressing myc-tagged Lulu isoforms were analyzed by immunoblotting with an anti-myc antibody. We confirmed that the expression of these proteins was efficiently induced by Dox removal. Comparative amounts of proteins were examined (α -tubulin was loading control). (D) MDCK Tet-Off cells, which can inducibly express myc-tagged Lulu1-L or Lulu2-S, were mixed with parental cells; expression was induced by removing Dox. Cells were doubly stained for myc and ZO-1. Arrows, apical constricted cells; arrowheads, basal protrusions. Lulu-expressing cells exhibit apical constriction. (E) Quantification of apical areas in Lulu1-L- or Lulu2-S-expressing cells and neighboring parental cells. The results obtained from two independent experiments are shown. Error bars indicate s.d. ($n > 50$). $**P < 0.001$ by Student's *t*-test. Scale bars: 20 μ m.

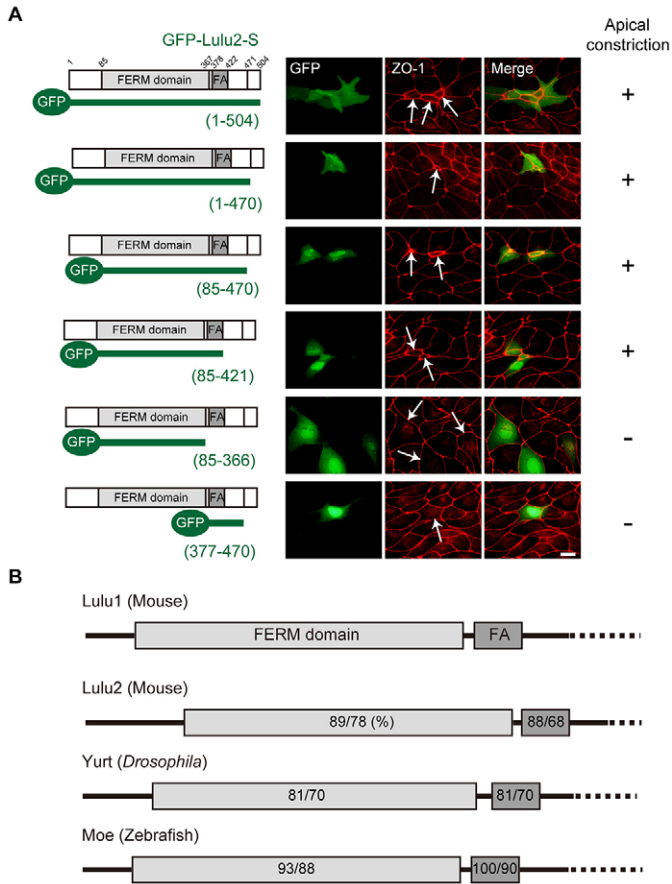


Fig. 3. Both FERM and FA domains are necessary and sufficient for inducing apical constriction. (A) GFP-tagged various mutant forms of Lulu2-S were transiently expressed in MDCK cells. Amino acid numbers of mouse Lulu2-S are indicated. Cells were doubly immunostained for GFP and ZO-1. All images were made by focusing ZO-1. GFP-Lulu2-S 85-470, 85-421, 85-366 and 377-470 tend to exhibit nuclear localization as well as cytoplasmic and lateral membrane localization. (B) FERM and FA domains are conserved not only between Lulu1 and Lulu2, but also across species. The numbers indicate similarities or identities of the domains compared with Lulu1 (left or right, respectively).

among Lulu subtypes. Lulu molecules commonly have a FERM and FA domain: the former is found in several other molecules and is well known to interact with lipids or proteins, whereas the latter exists in a restricted number of FERM-containing molecules and is thought to regulate the FERM domain, although its precise function is not fully understood (Baines, 2006; Bretscher et al., 2002). In addition, they commonly have a PDZ (post synaptic density protein, *Drosophila* disc large tumor suppressor and zonula occludens-1 protein)-domain binding motif in their C-terminal portions. Other than FERM and FA domains, there is no obvious homology between Lulu1 and Lulu2. We first tested the possible involvement of the PDZ-binding motif by examining a C-terminal-deleted mutant (amino acids 1-470), and found that the motif is not necessary for activity. Deletion of the portion of the N-terminus to the FERM domain (amino acids 1-84) also did not reduce activity. We further found that the mutant molecule consisting of only the FERM and FA domain (amino acids 85-421) exhibited potent activity to drive apical constriction. Interestingly, either the FERM

or FA domain alone did not have the ability to drive apical constriction. We obtained essentially the same results for Lulu1-L (our unpublished data). As the FERM and FA domains are highly conserved not only among Lulu subtypes but also across species (Fig. 3B), the activity of Lulu molecules on cell shape might be evolutionarily conserved.

Lulu induced lateral elongation in epithelial cells

Lateral elongation is often accompanied by apical constriction during morphogenesis (Lee, C. et al., 2007; Shook and Keller, 2003); therefore, to test whether the expression of Lulu proteins resulted in lateral elongation, we measured the cell heights of Lulu-expressing cells in mixed cell cultures. By labeling lateral membranes with an anti- β -catenin antibody, cell heights were found to be markedly increased in Lulu-expressing cells, indicating that Lulu proteins induce not only apical constriction, but also lateral elongation (Fig. 4A,B; our unpublished data). In addition, Lulu2-S-expressing cells exhibited longer cell protrusions than Lulu1 in the basal portion of cells (Fig. 2D, arrowheads), suggesting that Lulu2 again exhibits stronger activity with regards to lateral elongation than does Lulu1. It should be noted that β -catenin was localized continuously along the lateral membrane in Lulu-expressing cells, suggesting that the classic cadherin-based cell-cell junction was not disrupted by Lulu expression (Fig. 4A, arrows; 4B).

As cell-shape changes during morphogenesis often accompany changes in microtubule organization (Lee and Harland, 2007; Nakaya et al., 2008; Shook and Keller, 2003), we examined the distribution of microtubules in Lulu-expressing cells. In epithelial cells, including MDCK cells, microtubules are organized into lateral bundles, and apical and basal web-like networks (Bacallao et al., 1989; Reilein and Nelson, 2005; Reilein et al., 2005). The amounts of lateral bundles and of basal webs of microtubules, both of which were clearly observed in non-expressing neighboring cells (Fig. 4C, arrowheads), were significantly reduced in Lulu-expressing cells. In Lulu-expressing cells, apical microtubule webs seemed to remain intact, whereas the number of basolateral microtubules was reduced (Fig. 4C, arrows). These results clearly indicate that Lulu proteins commonly act to drive cell-shape change, i.e. a cuboidal to bottle-shaped morphological change (Fig. 4D), which is observed in ingressing cells during gastrulation.

Lulu proteins induce epithelial cell-shape change in a myosin-II-dependent manner

During morphogenetic processes, myosin-II is thought to be the major driving force in generating apical constriction in epithelial cells (Lecuit and Lenne, 2007; Lee and Harland, 2007; Martin et al., 2009). We therefore examined whether the Lulu-induced cell-shape change is associated with changes in the organization of the myosin-II network. Staining for myosin-IIA or -IIB revealed that both significantly accumulated along apical cell-cell boundaries in Lulu-expressing cells, whereas in non-expressing neighboring cells, they were mainly localized along stress fibers and scarcely found at cell-cell borders (Fig. 5A,B, supplementary material Fig. S3A,B). In addition, besides cell-cell boundaries, the intensity of myosin-II staining was often widely upregulated in Lulu-expressing cells compared with non-expressing cells (Fig. 5A, supplementary material Fig. S3A,B). Total protein levels of myosin-IIA or -IIB in Lulu-expressing cells were not significantly upregulated compared with non-expressing cells (supplementary material Fig. S3C), suggesting that myosin-II accumulation along cell-cell boundaries

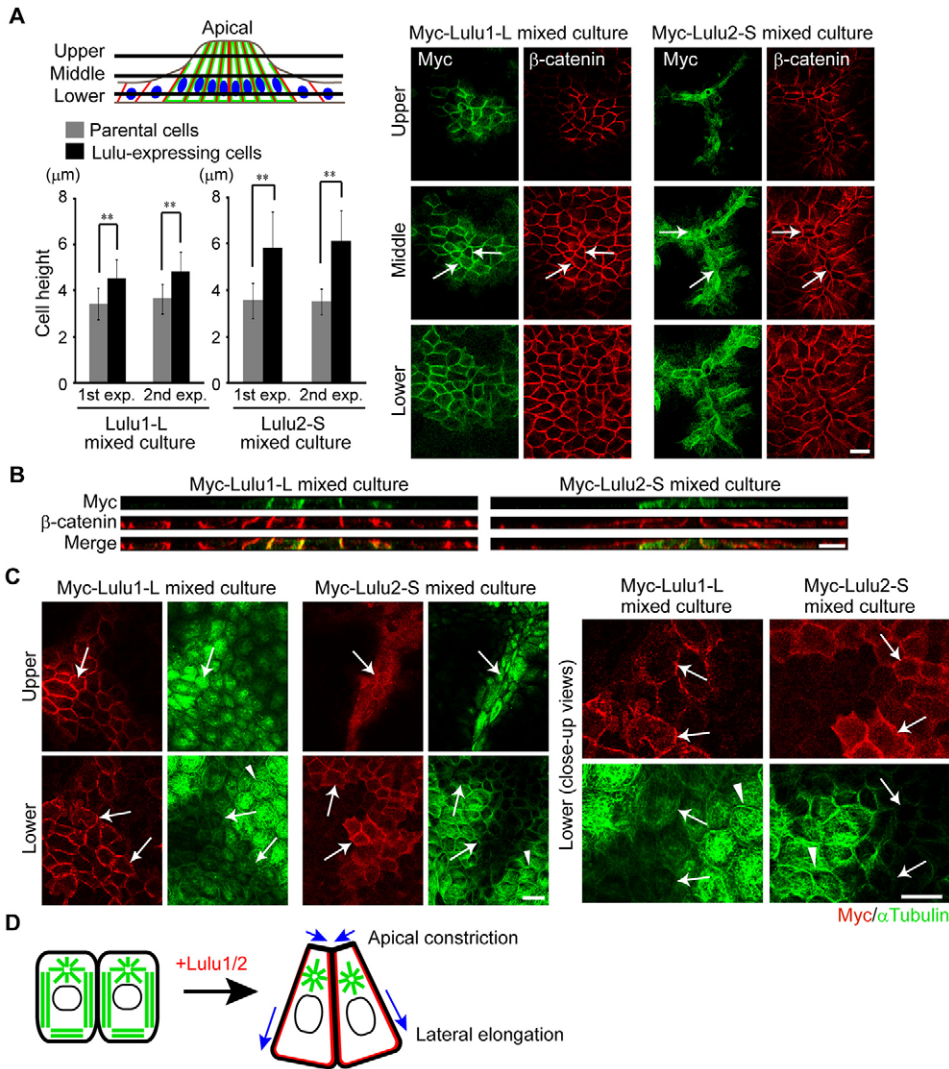


Fig. 4. Lulu induces lateral elongation and a change in microtubule organization.

(A) Confocal images of cells stained for β -catenin and myc at upper, middle or lower levels. The graph shows the cell heights of Lulu1-L- or Lulu2-S-expressing cells or parental cells. The results from two independent experiments are shown. Error bars indicate s.d. ($n > 50$ cells). $**P < 0.001$ by Student's *t*-test. Lulu-expressing cells exhibit lateral elongation. Note that β -catenin is detected normally in Lulu-expressing cells (arrows). (B) Mixed-cell cultures of parental and myc-tagged Lulu1-L- or Lulu2-S-expressing cells were doubly immunostained for β -catenin and myc. Vertical images of cells are shown. In Lulu-expressing cells, cell heightening and lateral elongation were observed. (C) Confocal images of cells doubly immunostained for α -tubulin and myc in upper and lower levels. Basolateral microtubules were reduced in Lulu-expressing cells (lower arrows). Arrowheads, lateral microtubule bundles and basal microtubule webs in parental cells; upper arrows, apical microtubule webs in Lulu-expressing cells. Close-up views are shown on the right. (D) Lulu1 and Lulu2 induce cell-shape changes that accompany apical constriction and lateral elongation. Green, microtubule; red, Lulu1 or Lulu2. Scale bars: 20 μm (A,C), 10 μm (B).

in Lulu-expressing cells might be due to local recruitment, not due to total upregulation of their protein levels. F-actin is also concentrated along the cell-cell boundaries of expressing cells, indicating that the myosin-II-F-actin network is upregulated in the apical portion of Lulu-expressing cells (Fig. 5C, supplementary material Fig. S3D).

Next, to address the role of myosin-II in Lulu-induced cell-shape change, we examined the effects of blebbistatin, a myosin-II-specific inhibitor, on Lulu-induced cell-shape change. When mixed-cell cultures were treated with blebbistatin, apical constriction became significantly impaired and apical areas of Lulu-expressing cells became almost identical to those of their non-expressing neighbors (Fig. 6A,B). Interestingly, the apical areas of non-expressing cells following blebbistatin treatment became smaller than before treatment, suggesting that the myosin-II-driven apical constriction of Lulu-expressing cells might pull the apical areas of non-expressing neighbors (Fig. 6A). The lateral elongation of Lulu-expressing cells also returned to normal, as determined by measuring their cell heights (Fig. 6C). Additionally, the microtubule organization of Lulu-expressing cells also returned to normal as a result of blebbistatin treatment (Fig. 6D). By contrast, treatment with paclitaxel or nocodazole (microtubule stabilizing and de-

stabilizing agents, respectively) did not alter the extent of apical constriction induced by Lulu proteins, suggesting that changes to microtubule organization might not be the cause of cell-shape change (our unpublished data). These results clearly indicate that myosin-II activity might serve as the major driving force of Lulu-induced cell-shape change in epithelial cells.

Rock participates in the upregulation of myosin-II by Lulu proteins

Myosin-II activity is upregulated mainly by the phosphorylation of MRLC singly at Thr18 or doubly at Thr18 and Ser19, which is mediated directly or indirectly by several kinases, including Rock, myosin light chain kinase (MLCK), MRCK and Citron kinase (Matsumura and Hartshorne, 2008). To test the involvement of MRLC phosphorylation in Lulu-induced apical constriction, we examined the localization of phosphorylated forms of MRLCs in Lulu-expressing cells of mixed-cell cultures. In Lulu-expressing cells, both mono-phosphorylated MRLC (1P-MRLC) and di-phosphorylated MRLC (2P-MRLC) strongly accumulated along apical cell-cell boundaries, compared with non-expressing neighbors (Fig. 7, supplementary material Fig. S4A). Fold increases of fluorescent intensities of 1P-MRLC, 2P-MRLC and ZO-1 along

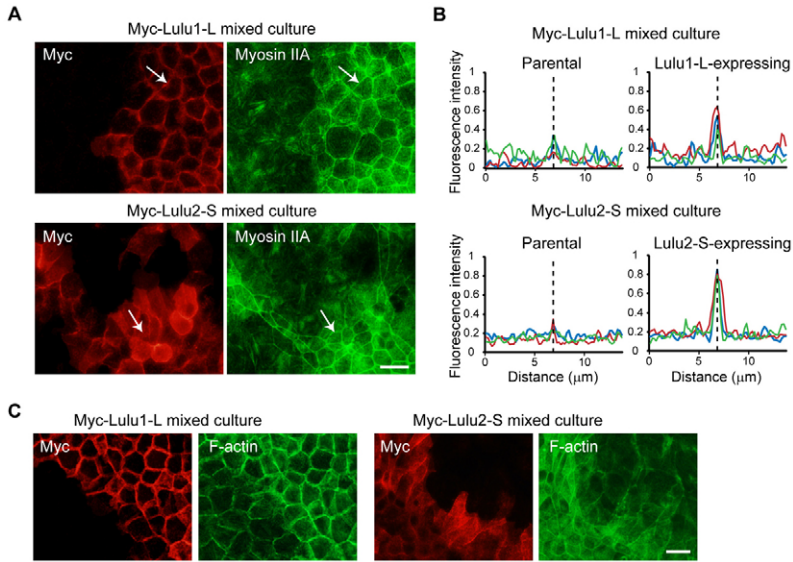


Fig. 5. Myosin-II and F-actin accumulate at the apical cell cortex in Lulu-expressing cells. (A) Mixed-cell cultures of parental and myc-tagged Lulu1-L- or Lulu2-S-expressing MDCK Tet-OFF cells were doubly immunostained for myosin-IIA and myc. Myosin-IIA accumulates along apical cell-cell boundaries in Lulu-expressing cells (arrows). (B) Fluorescence intensity of myosin-IIA signal scanned across apical cell-cell boundaries (indicated by dotted lines) of parental cells and Lulu-expressing cells. (C) Mixed-cell cultures of parental and myc-tagged Lulu1-L- or Lulu2-S-expressing MDCK Tet-OFF cells were doubly stained for myc and F-actin. F-actin accumulates along cell-cell boundaries. Scale bars: 20 μ m.

cell-cell boundaries in Lulu-expressing cells compared with those in parental cells showed that the signal of 1P- or 2P-MRLC was significantly upregulated compared with that of ZO-1, indicating that the accumulation of phosphorylated MRLC along cell-cell boundaries is not due to general upregulation of apical components

in apical-constricting cells, but to a positive regulatory mechanism underlining Lulu proteins (supplementary material Fig. S4B). Total levels of 1P- and 2P-MRLC examined by western blotting were also upregulated in Lulu-expressing cells, suggesting that phosphorylation of MRLC was enhanced by Lulu expression

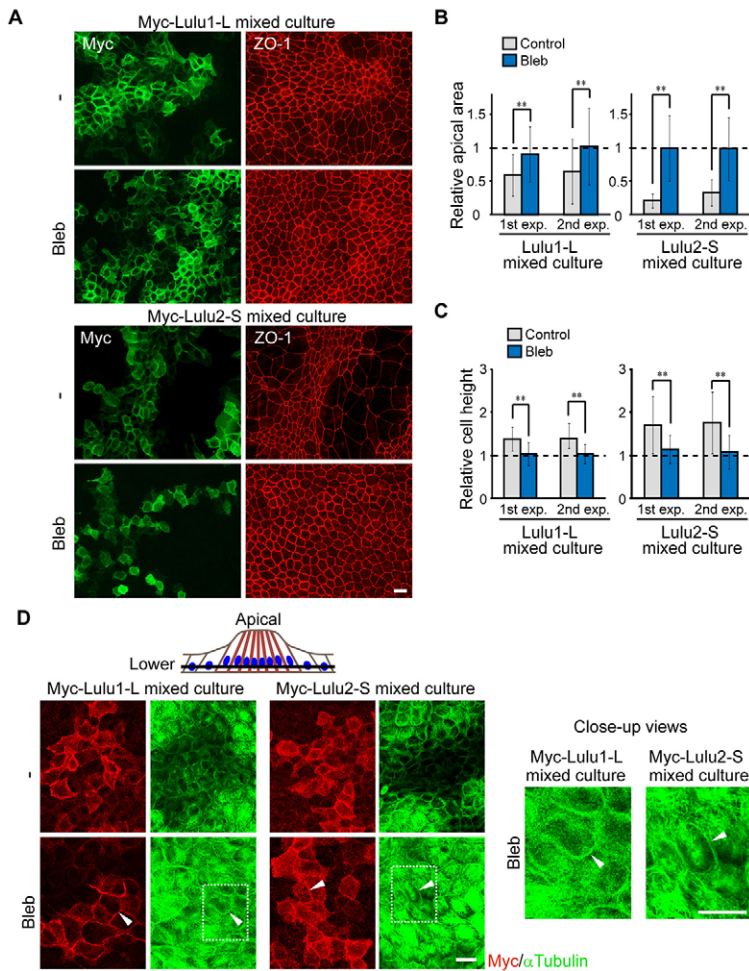


Fig. 6. Lulu-driven cell-shape change depends on myosin-II activity. (A-C) Mixed-cell cultures were treated with or without 100 μ M blebbistatin for 2 hours. Cells were doubly immunostained for ZO-1 and myc (A). Relative apical area (B) or relative cell heights (C) in Lulu-expressing cells, normalized by those in neighboring cells, were measured. Apical sizes and cell heights returned to normal following blebbistatin treatment. (D) Mixed-cell cultures doubly immunostained for α -tubulin and myc. By treating with blebbistatin, microtubule organization returned to normal in Lulu-expressing cells (arrowheads). Close-up views are shown on the right. Error bars indicate s.d. ($n > 50$ cells). $**P < 0.001$ by Student's *t*-test. Scale bars: 20 μ m.

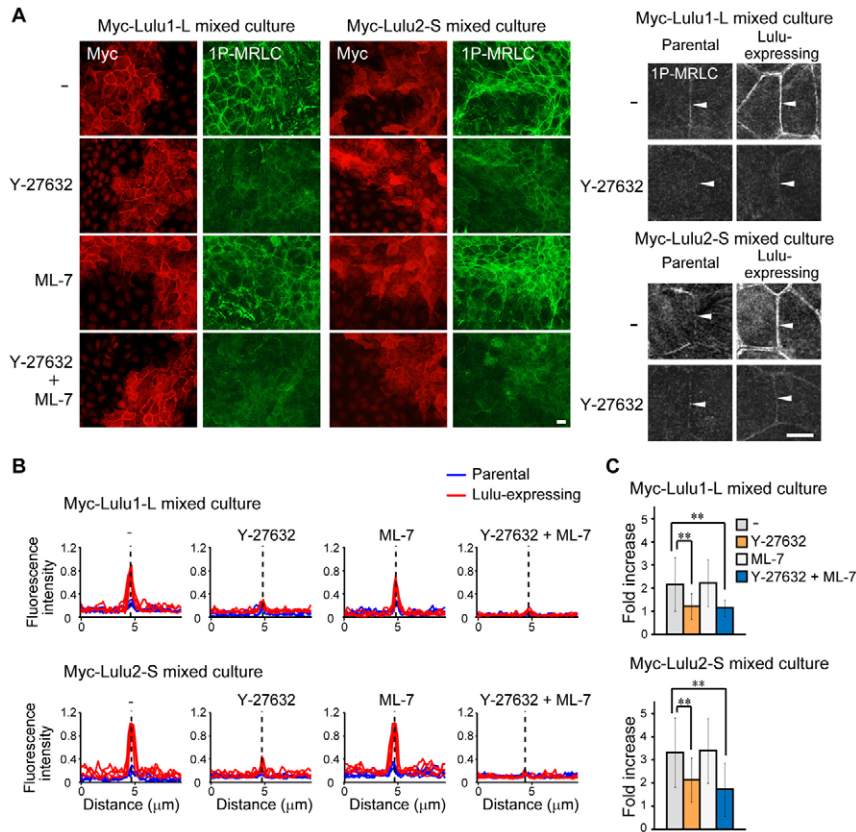


Fig. 7. Rock is involved in upregulation of myosin-II by Lulu proteins. (A) Mixed-cell cultures of parental and myc-tagged Lulu1-L- or Lulu2-S-expressing MDCK cells were treated with 20 μ M Y-27632 and/or 22 μ M ML-7 for 2 hours. Cells were doubly immunostained for 1P-MRLC and myc. Right panels show enlarged confocal images at apical cell-cell boundaries of cells. (B) Fluorescence intensity of the 1P-MRLC signal scanned across apical cell-cell boundaries (indicated by dotted lines) in parental or Lulu-expressing cells. (C) Fold increases of fluorescence intensities of the 1P-MRLC signal are shown scanned across apical cell-cell boundaries in Lulu-expressing cells, compared with those in neighboring cells. Error bars indicate s.d. ($n > 50$ cells). ** $P < 0.001$ by Student's *t*-test. Scale bars: 20 μ m (A, left), 10 μ m (A, right).

(supplementary material Fig. S3C). To explore the molecular mechanisms leading to the phosphorylation of MRLC, we examined the effects of the inhibitors on two upstream kinases, Rock and MLCK. When mixed-cell cultures were treated with Y-27632, a Rock inhibitor, the signal intensities of 1P- and 2P-MRLC staining in Lulu-expressing cells were markedly reduced at apical cell-cell boundaries (Fig. 7, supplementary material Fig. S4A), although the treatment did not completely eliminate the signals. By simultaneous treatment with Y-27632 and ML-7, an MLCK inhibitor, the signals of 1P- and 2P-MRLC staining in Lulu-expressing cells were further eliminated (Fig. 7, supplementary material Fig. S4A). By contrast, treatment with ML-7 alone did not markedly reduce the intensity of 1P-MRLC staining (Fig. 7). In contrast to 1P-MRLC, ML-7-treatment has some reducing effects on 2P-MRLC (supplementary material Fig. S4A). These results indicate that Rock is the major kinase responsible for MRLC phosphorylation downstream of Lulu proteins, and that MLCK also has some minor roles in MRLC phosphorylation.

Rock and MLCK are partially involved in Lulu-driven cell-shape change

Next, we examined the effects of the inhibitors on the Lulu-induced cell-shape change. The apical constriction induced by Lulu proteins was partially but markedly inhibited by treatment with Y-27632, and more efficiently by simultaneous treatment with Y-27632 and ML-7, whereas ML-7 treatment alone prompted little or no effect on the changes (Fig. 8A,B). The lateral elongation was also partially inhibited by simultaneous treatments with Y-27632 and ML-7 (Fig. 8C). These results strongly suggest that Rock and MLCK participate in the cell-shape change induced by

Lulu proteins, although MLCK seems to play only a minor role. The inhibitory effects of Y-27632 and ML-7 treatments were not as potent as those of blebbistatin treatment (compare Figs 6 and 8). This might be because of some additional mechanisms that activate myosin-II downstream of Lulu, or because the dephosphorylation of MRLC could not halt myosin-II activity during our experimental period.

Lulu proteins regulate the Rock–myosin-II axis in the basolateral portion of the cells

As treatment with blebbistatin inhibited not only apical constriction but also lateral elongation in Lulu-expressing cells, we examined the possible involvement of myosin-II in Lulu-driven lateral elongation. As expected, myosin-II was strongly accumulated in the basal portion of Lulu-expressing cells, often overlapping Lulu proteins (Fig. 9A). 1P-MRLC was also concentrated in the basal portion of Lulu-expressing cells, suggesting that myosin-II is activated there. Treatment with Y-27632 markedly reduced the staining intensity of 1P-MRLC, indicating that the phosphorylation of MRLC is a Rock-dependent event (Fig. 9B,C). These results clearly show that the Rock–myosin-II axis is activated not only in the apical portion but also in the basolateral portion of Lulu-expressing cells.

Shroom3 is not involved in Lulu-driven apical constriction

Shroom3 drives apical constriction via the Rock–myosin-II axis, as do Lulu proteins (Hildebrand and Soriano, 1999; Hildebrand, 2005; Nishimura and Takeichi, 2008). We thus examined whether Shroom3 is involved in apical constriction driven by Lulu proteins. Shroom3 was localized along the apical cell-cell boundaries marked

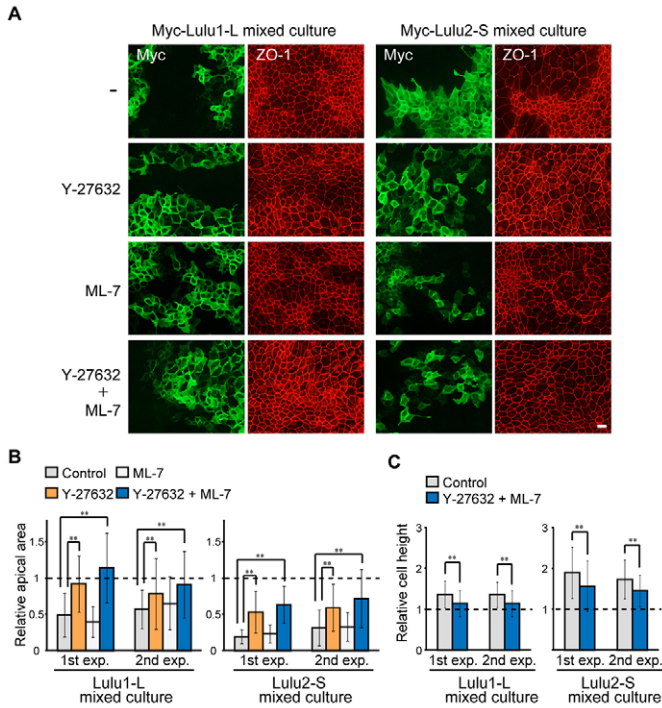


Fig. 8. Rock and MLCK participate in Lulu-induced cell-shape change. Mixed cell cultures of parental and myc-tagged Lulu1-L- or Lulu2-S-expressing cells were treated with Y-27632 and/or ML-7 for 2 hours. (A) Cells were doubly immunostained for myc and ZO-1. Apical constriction is partially inhibited by treatment with Y-27632 alone or simultaneous treatment with Y-27632 and ML-7. (B,C) Relative apical areas (B) and relative cell heights (C) were measured as in Fig. 6B and C, respectively ($n > 50$ cells). Lulu-driven cell-shape change is partially inhibited by treatment with Y-27632 alone or simultaneous treatment with Y-27632 and ML-7. Error bars indicate s.d. ($n > 50$ cells). ** $P < 0.001$ by Student's t test. Scale bar: 20 μm .

by ZO-1 in MDCK Tet-Off cells, although the expression levels of Shroom3 protein seemed to be low (Fig. 10A). Shroom3 was efficiently knocked-down by siRNA treatment, and its staining signal along cell-cell boundaries was almost completely lost in knocked-down cells (Fig. 10B,C). Shroom3 RNAi, however, did not inhibit the apical constriction of Lulu-expressing cells (Fig. 10D,E). Furthermore, neither 1P- nor 2P-MRLC accumulation along cell-cell boundaries in Lulu-expressing cells was significantly affected by *Shroom3* siRNA treatment (Fig. 10F,G; supplementary material Fig. S6). We obtained essentially the same results by examining two different siRNA sequences, confirming the specific effects of Shroom3 knockdown. These results strongly suggest that Lulu proteins induce apical constriction independently of Shroom3.

Lulu1-L is essential for proper organization of myosin-II-F-actin networks in epithelial cells

Among several epithelial cells, we found that NRK52E cells (rat renal epithelial cells) highly expressed Lulu1-L (Fig. 11A,B). In NRK52E cells, Lulu1-L was mainly detected along cell-cell boundaries (Fig. 11A). To examine the function of Lulu1-L in NRK52E cells, we conducted RNAi experiments. Lulu1-L was efficiently knocked down by our siRNA treatments, and staining signals for Lulu1-L along cell-cell boundaries were almost completely lost in knocked-down cells (Fig. 11C,D). In control cells,

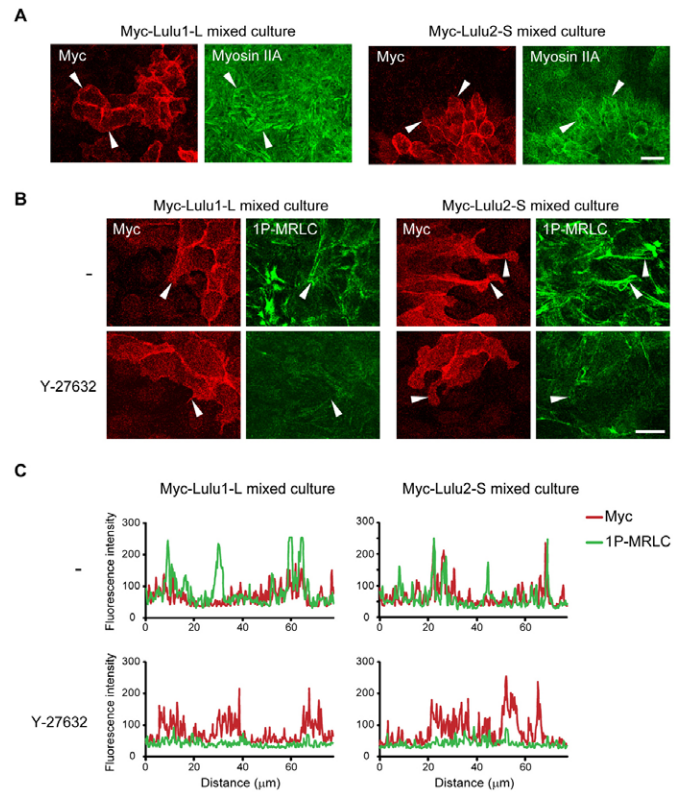


Fig. 9. Myosin-II is activated in the basal portion of Lulu-expressing cells. (A) Mixed-cell cultures of parental and myc-tagged Lulu1-L- or Lulu2-S-expressing MDCK cells were doubly immunostained for myc and myosin-IIA. Myosin-IIA is accumulated in the basal portion of Lulu-expressing cells (arrowheads). (B) Mixed cell cultures of parental and myc-tagged Lulu1-L- or Lulu2-S-expressing cells were left untreated or treated with Y-27632. The cells were doubly immunostained for myc and 1P-MRLC. 1P-MRLC was concentrated in the basal portion of Lulu-expressing cells, which is markedly reduced by treatment with Y-27632 (arrowheads). (C) Fluorescence intensity of myc or 1P-MRLC signal scanned in the basal plane of the mixed cell culture with or without Y-27632. Scale bars: 20 μm .

myosin-IIA and -IIB displayed multiple bundles of fibrous structures along cell-cell boundaries (Fig. 11E,F). By contrast, in Lulu1-L-depleted cells, such fibrous structures were completely lost (Fig. 11E,F; supplementary material Fig. S5). Similar to myosin-II, F-actin was also detected as multiple bundles along cell-cell boundaries in control cells. By contrast, such F-actin structures completely disappeared in Lulu1-L-depleted cells; instead, aberrant aggregates of F-actin were often observed in the centers of cells (Fig. 11G; supplementary material Fig. S5). Furthermore, β -catenin, a lateral marker, became discontinuously localized at cell-cell boundaries in Lulu1-L-depleted cells (Fig. 11H, supplementary material Fig. S5). In addition, ZO-1, a tight junctional marker, also became discontinuously localized at cell-cell boundaries in Lulu1-L-depleted cells (Fig. 11I, supplementary material Fig. S5). We obtained essentially the same results by examining three different siRNA sequences, confirming the specific effects of Lulu1-L knockdown (see supplementary material Fig. S5). These results strongly suggest that Lulu1-L maintains the integrity of lateral domain organization in NRK52E cells by regulating myosin-II-F-actin organization beneath lateral plasma membranes.

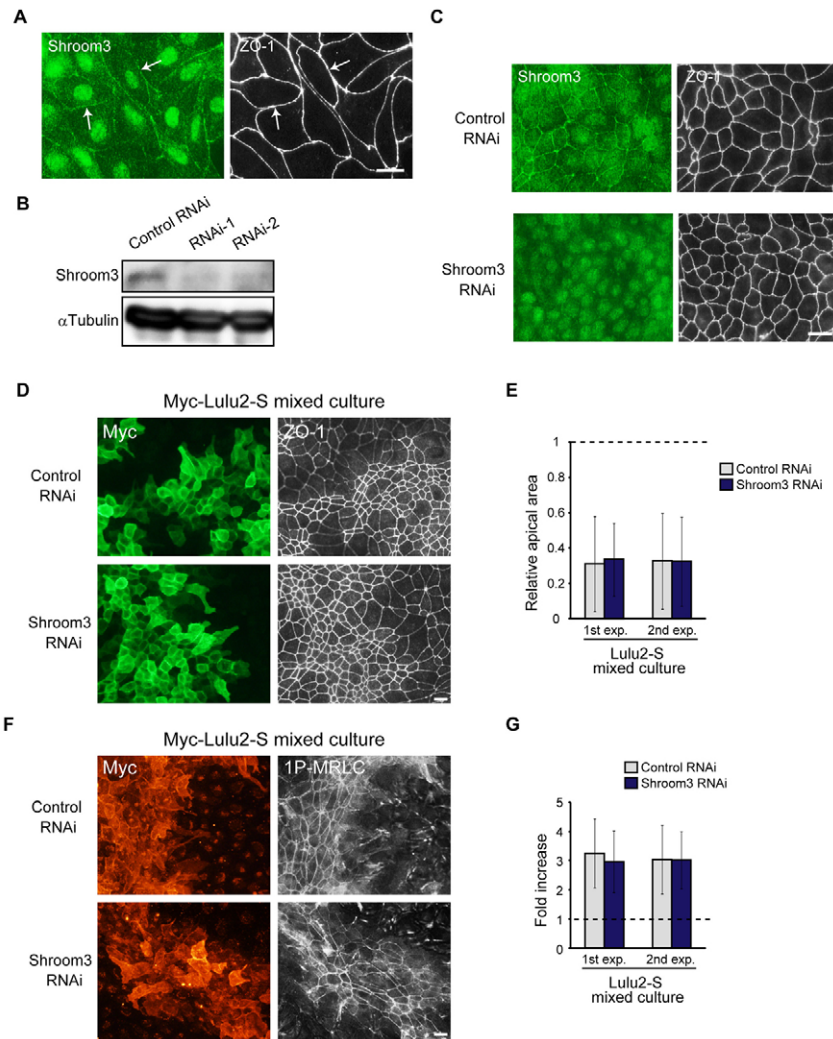


Fig. 10. Shroom3 is not involved in Lulu-driven apical constriction. (A) MDCK Tet-Off cells were doubly stained for Shroom3 and ZO-1. Shroom3 overlaps ZO-1. The nuclear signal is non-specific. (B) MDCK Tet-Off cells were transfected with control or *Shroom3* siRNAs and then analyzed by immunoblotting with the anti-Shroom3 antibody. Two different siRNAs efficiently knocked down Shroom3 expression. As essentially the same results were obtained, the results using RNAi-1 are shown in this figure. (C) MDCK Tet-Off cells treated with control siRNA or *Shroom3* siRNA were doubly immunostained for Shroom3 and ZO-1. Shroom3 was efficiently knocked down by treatment with *Shroom3* siRNA. (D) Mixed cell cultures of parental and myc-tagged Lulu2-S-expressing cells were treated with control or *Shroom3* siRNA. Cells were doubly stained for myc and ZO-1. Apical constriction of Lulu-expressing cells was not inhibited by Shroom3 knockdown. (E) Quantification of apical areas in Lulu2-S-expressing cells and neighboring parental cells treated with control or *Shroom3* siRNA. Results obtained from two independent experiments are shown. (F) Mixed cell cultures of parental and myc-tagged Lulu2-S-expressing cells were treated with control or *Shroom3* siRNA. Cells were doubly stained for myc and 1P-MRLC. Shroom3 knockdown did not affect the accumulation of 1P-MRLC along apical cell-cell boundaries. (G) Fluorescent intensity of the 1P-MRLC signal scanned across apical cell-cell boundaries (indicated by dotted lines) in parental or Lulu-expressing cells treated with control or *Shroom3* siRNA. Error bars in E and G indicate s.d. ($n > 50$ cells). Scale bars: 20 μ m.

Discussion

We show here that Lulu1 and Lulu2 commonly exhibit activities that change epithelial cells from cuboidal to bottle-like morphology. This cell-shape change is crucial to the involution, invagination and bending of epithelial cell sheets during animal morphogenesis. We further present evidence that Lulu-driven cell-shape change is caused by the upregulation of myosin-II at the cell cortex, and that the phosphorylation of myosin regulatory light chain is mainly mediated by Rock. Additionally, Lulu1 RNAi in epithelial cells resulted in mislocalization of myosin-II with the concomitant loss of proper lateral organization, supporting the notion that Lulu proteins primarily regulate myosin-II. Lulu proteins activate myosin-II independently of Shroom3, another well-known regulator of apical constriction during morphogenesis. We further found that both FERM and FA domains of Lulu proteins are necessary and sufficient for Lulu-driven apical constriction. As both domains are highly conserved not only among Lulu subtypes but also across species, the activity of Lulu on myosin-II might be conserved across species.

Lulu1 mutant mice were reported to exhibit defects in shaping ingressing cells during gastrulation: Although ingressing cells normally exhibited a bottle-shaped morphology, the cells in mutant mice displayed a rounded morphology (Lee, J. D. et al., 2007). In

another previous report, it was proposed that Lulu1 regulates the state of classic cadherins and integrins, and that their misregulation might be responsible for defects in gastrulation in mutants (Hirano et al., 2008). We here present a different explanation for the mutant phenotype: Lulu1 might primarily maintain the proper organization and activation of myosin-II in ingressing cells, and it is the misregulation of myosin-II that is responsible for the mutant phenotype.

In a previous report, it was shown that Lulu1 negatively regulates the E-cadherin level via competitively binding to p120 catenin (Hirano et al., 2008). If Lulu generally plays such a role, the expression of Lulu in epithelial cells should lead to the disruption or weakening of the cell-cell junction, and loss of Lulu expression in the cells might strengthen the cell-cell junction. However, our data include contradictory results: on the one hand, Lulu1-expression in MDCK cells did not disrupt the cell-cell junction; and on the other hand Lulu1-RNAi in NRK52E cells did not enhance the cell-cell junction, but disrupted it. Furthermore, we could not detect significant alternation in protein levels of E-cadherin or α -catenin, β -catenin and p120 by Lulu expression (see supplementary material Fig. S7). From these results, we conclude that Lulu1 might not generally function to downregulate E-cadherin. In the previous report, Lulu1 was shown to localize at focal contacts by interacting

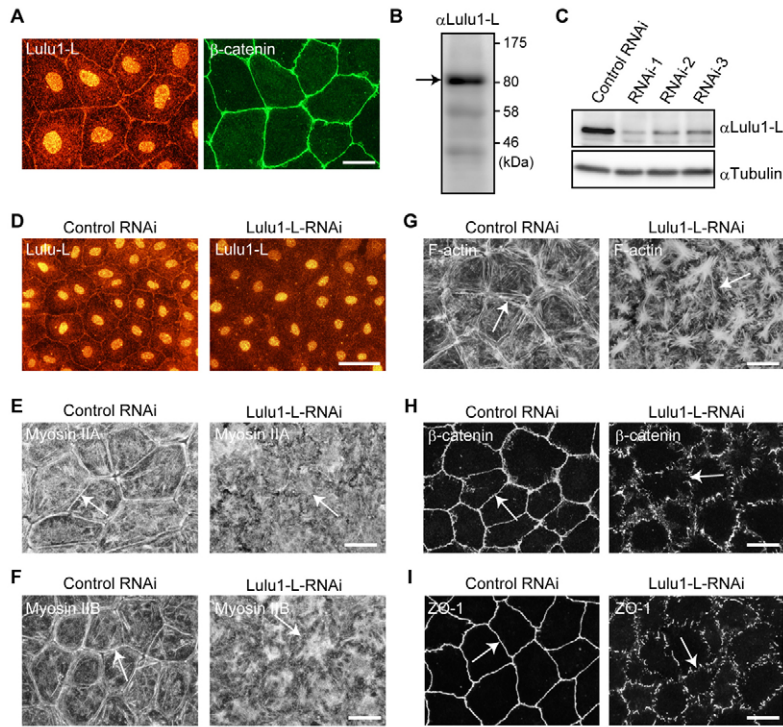


Fig. 11. Lulu1-L is essential for myosin-II-F-actin organization in NRK52E cells. (A) NRK52E cells doubly immunostained for Lulu1-L and β -catenin. Lulu1-L is localized along cell-cell boundaries overlapping β -catenin. The nuclear signal is non-specific. (B) Immunoblotting to detect Lulu1-L in NRK52E cells. (C) NRK52E cells were transfected with control or *Lulu1-L* siRNAs and then analyzed by immunoblotting with the anti-Lulu1-L antibody. Three different siRNAs efficiently knocked down Lulu1-L expression. (D-I) NRK52E cells treated with control or Rat *Lulu1-L-1* siRNAs were immunostained for Lulu1-L (D), myosin-IIA (E), myosin-IIB (F), F-actin (G), β -catenin (H), or ZO-1 (I). Arrows, cell-cell boundaries (E-I). Lulu1-L depletion resulted in the disorganization of myosin-II-F-actin networks and lateral organization. Scale bars: 25 μ m (A,E-I), 50 μ m (D).

with paxillin, thus enhancing the turnover of focal contacts (Hirano et al., 2008); however, in our experimental conditions, we could not detect either endogenous or exogenous Lulu1 at focal contacts. Thus, the localization of Lulu1 at focal contacts might be a cell-type-specific event. Our proposal and the previous one concerning cadherin and integrin might not be mutually exclusive; further study is needed to clarify in more detail the mechanisms underlying Lulu regulation of cell-shape change.

Moe and Yurt (zebrafish and *Drosophila* Lulu proteins, respectively) were reported to interact with and negatively regulate Crumbs, an apical membrane regulator, thus restricting the apical domain during morphogenesis (Hsu et al., 2006; Laprise et al., 2006). We found here, however, that mammalian Lulu molecules primarily function to upregulate myosin-II activity, which might not be caused by downregulation of Crumbs because, in Lulu2-S expressing cells, the staining signal of apically located Crb3 (a member of vertebrate Crumbs) was not reduced, but significantly enhanced (supplementary material Fig. S2D). Lulu-mediated negative regulation of Crumbs might therefore take place in specific developmental contexts. The linkage between Lulu and Crumbs is most obvious in photoreceptor cells in both zebrafish and *Drosophila* (Hsu et al., 2006; Laprise et al., 2006) and it will be interesting to explore the function of Lulu proteins in mammalian photoreceptor morphogenesis, where Lulu might regulate Crumbs.

How do Lulu proteins upregulate myosin-II? Rock is well known to regulate the epithelial architecture during morphogenesis, including apical constriction (Dawes-Hoang et al., 2005; Escudero et al., 2007; Hildebrand, 2005). We here identified Rock as the major kinase in the phosphorylation of MRLC downstream of Lulu proteins. Rock indeed plays a role in cell-shape change induced by Lulu proteins because the Rock inhibitor has a clear but moderate effect on the change. Shroom3, another regulator of myosin-II during vertebrate morphogenesis, seems to function mainly as an activator of Rock because it recruits Rock at the position of the apical junction by

directly binding to Rock (Hildebrand, 2005; Nishimura and Takeichi, 2008). We showed here that Shroom3 is not involved in Lulu-driven apical constriction: the Lulu-myosin-II and Shroom3-myosin-II pathways are different signaling pathways. There might be more complicated molecular mechanisms downstream of Lulu proteins in regulating myosin-II than there are downstream of Shroom3, and they should be elucidated in future research.

During invagination and folding of the epithelial structures, lateral elongation is often, but not always, accompanied by apical constriction (Lee, C. et al., 2007; Lee and Harland, 2007). In contrast to apical constriction, the mechanisms of lateral elongation are poorly understood. Shroom family members again are known to drive not only apical constriction but also lateral elongation (Lee et al., 2009; Lee, C. et al., 2007). The latter is thought to be caused by Shroom-driven accumulation of γ -tubulin, a microtubule nucleating protein, at the apical surface of cells, although the precise mechanism of the accumulation has not been clarified. Lulu expression, however, did not change the distribution of γ -tubulin (data not shown), suggesting that other mechanisms regulate Lulu-driven lateral elongation. Our results show that myosin-II activity is required for both Lulu-induced apical constriction and lateral elongation, in good agreement with a recent report that myosin-II is necessary for apico-basal cell elongation to form a columnar cell shape in *Drosophila* wing disc epithelial cells (Widmann and Dahmann, 2009); therefore, there might be an evolutionarily conserved mechanism of myosin-II-driven lateral elongation. Very recently, Yurt was also shown to be localized in the basolateral portion of the cells during organogenesis, and play an essential role in apico-basal polarity maintenance (Laprise et al., 2009). Our results here also show that Lulu knockdown in NRK52E cells resulted in failure of proper formation of tight and adherens junctions, which can also be interpreted as a loss of apico-basal polarity. It, therefore, might be interesting to test whether myosin-II is also activated by Yurt during *Drosophila* organogenesis.

In addition to apical constriction and lateral elongation, Lulu induces a marked change in microtubule organization. Lateral bundles and basal webs of microtubules were significantly reduced in Lulu-expressing cells, although the apical microtubule web remained normal in the cells. Such a change in microtubule organization is also observed in ingressing cells during gastrulation (Nakaya et al., 2008), in which ingressing cells accumulate apical microtubules with a concomitant loss of basolateral microtubules. It will be interesting to test whether microtubule organization also changes in ingressing cells during gastrulation in Lulu mutant mice. We further showed here that myosin-II regulates microtubule organization change because microtubule organization in Lulu-expressing cells returned to normal after treatment with the myosin-II inhibitor. It would be interesting to address the roles of myosin-II in the changes in microtubule organization in ingressing cells during gastrulation.

Our analysis using mutant forms of Lulu identified the FA domain as a portion of Lulu necessary for driving apical constriction. FA domains are conserved in a restricted number of FERM-domain-containing molecules, including Lulu proteins, PTN3, Epb41, and Epb4111-Epb4113 (Baines, 2006). As the FA domain is not found in well-characterized FERM-domain-containing molecules such as merlin, moesin and ezrin, its roles have not been well understood. Our results here show, for the first time, the importance of the FA domain in protein activity, thus helping to elucidate the function of the FA domain.

Our knowledge of Lulu2 molecules in physiological contexts is limited. Lulu2 was reported to be upregulated in metastatic cancers, suggesting that it might play a role in cell migration or invasion (Shimizu et al., 2000; Wang et al., 2006), and the function of Lulu2 during animal morphogenesis has not been examined. Our results indicate that Lulu2 has more potent activity than Lulu1 with regards to cell-shape change. Where and how the strong activity of Lulu2 is utilized during morphogenesis are of particular interest for future study.

Our results show the novel and unexpected activity of Lulu proteins in myosin-II regulation. This activity resides in the conserved FERM and FA domains but it should be noted that the C-terminal portions of Lulu isoforms vary in their amino acid sequences, suggesting that each C-terminal portion might possess specific functions. Supporting this notion, the mammalian Lulu1-S and Lulu1-L, which commonly have FERM and FA domains, exhibited differences in their abilities to rescue zebrafish Moe mutants (Christensen and Jensen, 2008); therefore, we cannot rule out the possibility that Lulu1 and Lulu2 have non-overlapping activities. This is another interesting issue to be addressed in our future studies.

Materials and Methods

Cell culture and immunostaining

MDCK Tet-Off cells (Clontech) were cultured in a 1:1 mixture of DME and Ham's F12 medium (Iwaki), supplemented with 10% fetal calf serum. NRK52E cells (a rat renal epithelial cell line provided by Shigenobu Yonemura, RIKEN Center for Developmental Biology, Kobe, Japan) were cultured in DME (Nissui) containing 10% fetal calf serum. These cells were maintained in 5% CO₂ at 37°C. To isolate stable MDCK Tet-Off transfectants, 250 µg/ml hygromycin B (Invitrogen) was used. The stable MDCK Tet-Off transfectants were cultured in the presence of 1 µg/ml doxycycline (Dox). To induce Lulu molecules, the cells were washed twice at 12-hour intervals and cultured in Dox-free medium for 2-3 days. The following chemicals were used: blebbistatin (Sigma), Y-27632 (Calbiochem), ML-7 (Sigma) and Dox (Clontech). Cells were transfected using FuGENE reagent (Roche) according to the manufacturer's protocol. Immunostaining was performed as described previously (Tanoue and Takeichi, 2004); briefly, cells were fixed with 1% or 3.7% formaldehyde in PBS for 10 minutes at room temperature. For microtubule staining, cells were fixed with 4% PFA in PBS at pH 6.9 and 1 mM EGTA for 15 minutes at 37°C. The

fixed cells were then permeabilized with 0.2% Triton X-100 in PBS for 10 minutes and blocked with 3% BSA in PBS for 30 minutes at 37°C. Thereafter, the cells were incubated with appropriate antibodies in 3% BSA in PBS for 1.5 hours at 37°C. Next, the cells were washed three times with PBS and incubated with fluorochrome-conjugated secondary antibodies (1:400, Alexa Fluor secondary antibodies; Invitrogen) in 3% BSA in PBS for 1 hour at 37°C. After three washes with PBS and a rinse in Milli-Q water (Millipore), coverslips were mounted with Mowiol (Calbiochem). Alexa-Fluor-488-phalloidin (Invitrogen) was used to visualize F-actin. Images were analyzed with the same software and with Photoshop (Adobe). Apical area and cell height were quantified by counting pixels using ImageJ or LSM510 software, respectively. Apical area was defined as the area surrounded by ZO-1. Cell height was determined by β-catenin staining. Fluorescent intensities were measured by counting gradient values using ImageJ software.

Antibodies

Rabbit polyclonal antibody against Lulu1-L was raised against amino acids 669-731 of mouse Lulu1-L. The specificity of the antibody was confirmed by the observation that their immunostaining signals disappeared following RNAi-mediated depletion of Lulu1-L in NRK52E cells, as well as by transfection experiments (Fig. 10C,D; supplementary material Fig. S1A,B). Rabbit polyclonal Crb3 antibody was raised against amino acids 94-113 of mouse Crb3. The following antibodies were also used: mouse monoclonal antibodies against β-catenin (Transduction), ZO-1 (Invitrogen), 1P-MRLC (Cell Signaling), α-tubulin (DM1A; Sigma) and Myc (Santa Cruz Biotechnology); rat monoclonal antibody against GFP (Nacalai), and rabbit polyclonal antibodies against ZO-1 (Invitrogen), myosin-IIA (Sigma), myosin-IIB (Sigma), 2P-MRLC (Cell Signaling), Myc (MBL), Par3 (Upstate) and GFP (MBL). Rabbit anti-Shroom3 antibody was a gift from Jeffrey Hildebrand, University of Pittsburgh, Pittsburgh, PA. Primary antibodies were visualized with goat fluorochrome-conjugated secondary antibodies. The fluorochromes used were AlexaFluor 488, 555, and 568 (Invitrogen).

Plasmid construction and protein expression

Full-length mouse cDNA of Lulu1-S and Lulu1-L, and of Lulu2-L was obtained by PCR and then cloned into pEGFP-C1 (Clontech) or pTRE2hyg (Clontech), in which a 3×myc tag was attached to their N-terminus. Mouse cDNA of Lulu2-S was provided by Jun Yokota (National Cancer Center Research Institute, Tokyo, Japan). The pGEX-4T3 vector (GE Healthcare) was used to produce GST fused to amino acids 669-731 of Lulu1-L in *E. coli*.

RNAi

The following Stealth siRNAs (Invitrogen) were used for RNAi experiments: Rat *Lulu1-L-1*, 5'-UUAACUCGAAGAUGAAGACAAUAGG-3'; Rat *Lulu1-L-2*, 5'-AUCAAAGGGACACUCUUAACUCCCA-3'; Rat *Lulu1-L-3*, 5'-AUAAAUACCGGUUAGCUCCUCACG-3'; *Shroom3-1*, 5'-CCUAGAGCCUCAGCAGC-AAGUUA-3'; *Shroom3-2*, 5'-CAGAAAGACCUCAGAAGACAUCAGAA-3'. Stealth RNAi negative control (Invitrogen) was used for control RNAi. Transfection of Stealth siRNA was performed using RNAi MAX reagent (Invitrogen).

Immunohistochemistry

Tissue sectioning and immunohistochemical analysis were performed as described previously (Ishiyuchi et al., 2009); briefly, embryonic mouse organs were fixed in 1% or 4% PFA in PBS for 2-6 hours at 4°C. After serial incubation in 15, 20, and 30% sucrose in PBS at 4°C, the organs were mounted in OCT compound (SAKURA), frozen, and sectioned with a cryostat (Leica). The samples were made permeable in 0.2% TritonX-100 in PBS for 10 minutes at room temperature and blocked with 3% BSA in PBS for 30 minutes at 37°C. The samples were incubated with primary antibodies in 3% BSA in PBS for 1 hour at 37°C, followed by three washes with PBS. After incubation with secondary antibodies in 3% BSA in PBS for 1 hour at 37°C, and washing with PBS, the samples were mounted in Mowiol (Calbiochem).

Western blotting

Embryonic mouse organs or MDCK Tet-Off and NRK52E cells were homogenized or lysed in 20 mM Tris-HCl (pH 7.4) containing 1 mM MgCl₂, 2 mM EGTA, 150 mM NaCl, 0.5% Nonidet-40, and a protease inhibitor cocktail (Roche). Proteins were fractionated by SDS-PAGE using a 10% or 15% gel. The fractionated proteins were electroblotted onto Immobilon-P polyvinylidene difluoride membranes (Millipore) using semi-dry transfer apparatus (Bio-Rad Laboratories). The membrane was blocked with 5% skim milk or 2% ECL Advance blocking agent for 30 minutes at room temperature. Proteins were then probed for 16 hours at 4°C with an appropriate antibody in 20 mM Tris-HCl (pH 7.4) containing 150 mM NaCl and 3% BSA, or in 20 mM Tris-HCl (pH 7.4) containing 150 mM NaCl, 0.05% Tween 20 and 0.2% ECL Advance blocking agent. The membrane was then washed three times at room temperature (15 minutes each time) in 20 mM Tris-HCl (pH 7.4) containing 150 mM NaCl and 0.05% Tween 20 (TBS-Tween), and was subsequently incubated for 2 hours at room temperature with a secondary antibody in TBS-Tween containing 5% skim milk or 2% ECL Advance blocking agent. After three washes with TBS-Tween, the proteins were detected using the ECL plus reagent (PerkinElmer) or ECL Advance reagent (GE Healthcare), according to the manufacturer's protocol. Chemiluminescence was detected using an ImageQuant400 (GE Healthcare).

We are grateful to Yukako Oda, Masatoshi Takeichi and Tamako Nishimura for discussion, Misako Wakao and Phan Thuy Chau for technical support, Mikio Furuse for access to equipment, Jeffrey Hildebrand for anti-Shroom3 antibody and Jun Yokota for the cDNA of Lulu2-S. This work was supported by grants from the G-COE Program and Grant-in-Aid for Young Scientists (A) (to T.T.) and a grant for young researchers from the G-COE Program (to H.N.).

Supplementary material available online at

<http://jcs.biologists.org/cgi/content/full/123/4/555/DC1>

References

- Bacallao, R., Antony, C., Dotti, C., Karsenti, E., Stelzer, E. H. and Simons, K. (1989). The subcellular organization of Madin-Darby canine kidney cells during the formation of a polarized epithelium. *J. Cell Biol.* **109**, 2817-2832.
- Baines, A. J. (2006). A FERM-adjacent (FA) region defines a subset of the 4.1 superfamily and is a potential regulator of FERM domain function. *BMC Genomics* **7**, p. 85.
- Barrett, K., Leptin, M. and Settlemann, J. (1997). The Rho GTPase and a putative RhoGEF mediate a signaling pathway for the cell shape changes in *Drosophila* gastrulation. *Cell* **91**, 905-915.
- Bretscher, A., Edwards, K. and Fehon, R. G. (2002). ERM proteins and merlin: integrators at the cell cortex. *Nat. Rev. Mol. Cell Biol.* **3**, 586-599.
- Chauhan, S., Pandey, R., Way, J. F., Sroka, T. C., Demetriou, M. C., Kunz, S., Cress, A. E., Mount, D. W. and Miesfeld, R. L. (2003). Androgen regulation of the human FERM domain encoding gene EHM2 in a cell model of steroid-induced differentiation. *Biochem. Biophys. Res. Commun.* **310**, 421-432.
- Christensen, A. K. and Jensen, A. M. (2008). Tissue-specific requirements for specific domains in the FERM protein Moe/Epb4.115 during early zebrafish development. *BMC Dev. Biol.* **8**, p. 3.
- Costa, M., Wilson, E. T. and Wieschaus, E. (1994). A putative cell signal encoded by the folded gastrulation gene coordinates cell shape changes during *Drosophila* gastrulation. *Cell* **76**, 1075-1089.
- Dawes-Hoang, R. E., Parmar, K. M., Christiansen, A. E., Phelps, C. B., Brand, A. H. and Wieschaus, E. F. (2005). Folded gastrulation, cell shape change and the control of myosin localization. *Development* **132**, 4165-4178.
- Escudero, L. M., Bischoff, M. and Freeman, M. (2007). Myosin II regulates complex cellular arrangement and epithelial architecture in *Drosophila*. *Dev. Cell* **13**, 717-729.
- García-García, M. J., Eggenschwiler, J. T., Caspary, T., Alcorn, H. L., Wyler, M. R., Huangfu, D., Rakeman, A. S., Lee, J. D., Feinberg, E. H., Timmer, J. R. et al. (2005). Analysis of mouse embryonic patterning and morphogenesis by forward genetics. *Proc. Natl. Acad. Sci. USA.* **102**, 5913-5919.
- Hacker, U. and Perrimon, N. (1998). DRhoGEF2 encodes a member of the Dbl family of oncogenes and controls cell shape changes during gastrulation in *Drosophila*. *Genes Dev.* **12**, 274-284.
- Haigo, S. L., Hildebrand, J. D., Harland, R. M. and Wallingford, J. B. (2003). Shroom induces apical constriction and is required for hinge point formation during neural tube closure. *Curr. Biol.* **13**, 2125-2137.
- Hildebrand, J. D. (2005). Shroom regulates epithelial cell shape via the apical positioning of an actomyosin network. *J. Cell Sci.* **118**, 5191-5203.
- Hildebrand, J. D. and Soriano, P. (1999). Shroom, a PDZ domain-containing actin-binding protein, is required for neural tube morphogenesis in mice. *Cell* **99**, 485-497.
- Hirano, M., Hashimoto, S., Yonemura, S., Sabe, H. and Aizawa, S. (2008). EPB41L5 functions to post-transcriptionally regulate cadherin and integrin during epithelial-mesenchymal transition. *J. Cell Biol.* **182**, 1217-1230.
- Hoover, K. B. and Bryant, P. J. (2002). *Drosophila* Yurt is a new protein-4.1-like protein required for epithelial morphogenesis. *Dev. Genes Evol.* **212**, 230-238.
- Hsu, Y. C., Willoughby, J. J., Christensen, A. K. and Jensen, A. M. (2006). Mosaic Eyes is a novel component of the Crumbs complex and negatively regulates photoreceptor apical size. *Development* **133**, 4849-4859.
- Ishuchi, T., Misaki, K., Yonemura, S., Takeichi, M. and Tanoue, T. (2009). Mammalian Fat and Dachsous cadherins regulate apical membrane organization in the embryonic cerebral cortex. *J. Cell Biol.* **185**, 959-967.
- Jensen, A. M. and Westerfield, M. (2004). Zebrafish mosaic eyes is a novel FERM protein required for retinal lamination and retinal pigmented epithelial tight junction formation. *Curr. Biol.* **14**, 711-717.
- Kolsch, V., Seher, T., Fernandez-Ballester, G. J., Serrano, L. and Leptin, M. (2007). Control of *Drosophila* gastrulation by apical localization of adherens junctions and RhoGEF2. *Science* **315**, 384-386.
- Laprise, P., Beronja, S., Silva-Gagliardi, N. F., Pellikka, M., Jensen, A. M., McGlade, C. J. and Tepass, U. (2006). The FERM protein Yurt is a negative regulatory component of the Crumbs complex that controls epithelial polarity and apical membrane size. *Dev. Cell* **11**, 363-374.
- Laprise, P., Lau, K. M., Harris, K. P., Silva-Gagliardi, N. F., Paul, S. M., Beronja, S., Beitel, G. J., McGlade, C. J. and Tepass, U. (2009). Yurt, Coracle, Neurexin IV and the Na(+),K(+)-ATPase form a novel group of epithelial polarity proteins. *Nature* **459**, 1141-1145.
- Lecuit, T. and Lenne, P. F. (2007). Cell surface mechanics and the control of cell shape, tissue patterns and morphogenesis. *Nat. Rev. Mol. Cell Biol.* **8**, 633-644.
- Lee, C., Scherr, H. M. and Wallingford, J. B. (2007). Shroom family proteins regulate gamma-tubulin distribution and microtubule architecture during epithelial cell shape change. *Development* **134**, 1431-1441.
- Lee, C., Le, M. P. and Wallingford, J. B. (2009). The shroom family proteins play broad roles in the morphogenesis of thickened epithelial sheets. *Dev. Dyn.* **238**, 1480-1491.
- Lee, J. D., Silva-Gagliardi, N. F., Tepass, U., McGlade, C. J. and Anderson, K. V. (2007). The FERM protein Epb4.115 is required for organization of the neural plate and for the epithelial-mesenchymal transition at the primitive streak of the mouse embryo. *Development* **134**, 2007-2016.
- Lee, J. Y. and Harland, R. M. (2007). Actomyosin contractility and microtubules drive apical constriction in *Xenopus* bottle cells. *Dev. Biol.* **311**, 40-52.
- Martin, A. C., Kaschube, M. and Wieschaus, E. F. (2009). Pulsed contractions of an actin-myosin network drive apical constriction. *Nature* **457**, 495-499.
- Matsumura, F. and Hartshorne, D. J. (2008). Myosin phosphatase target subunit: Many roles in cell function. *Biochem. Biophys. Res. Commun.* **369**, 149-156.
- Nakaya, Y., Sukowati, E. W., Wu, Y. and Sheng, G. (2008). RhoA and microtubule dynamics control cell-basement membrane interaction in EMT during gastrulation. *Nat. Cell Biol.* **10**, 765-775.
- Nishimura, T. and Takeichi, M. (2008). Shroom3-mediated recruitment of Rho kinases to the apical cell junctions regulates epithelial and neuroepithelial planar remodeling. *Development* **135**, 1493-1502.
- Pilot, F. and Lecuit, T. (2005). Compartmentalized morphogenesis in epithelia: from cell to tissue shape. *Dev. Dyn.* **232**, 685-694.
- Reilein, A. and Nelson, W. J. (2005). APC is a component of an organizing template for cortical microtubule networks. *Nat. Cell Biol.* **7**, 463-473.
- Reilein, A., Yamada, S. and Nelson, W. J. (2005). Self-organization of an acentrosomal microtubule network at the basal cortex of polarized epithelial cells. *J. Cell Biol.* **171**, 845-855.
- Shimizu, K., Nagamachi, Y., Tani, M., Kimura, K., Shiroishi, T., Wakana, S. and Yokota, J. (2000). Molecular cloning of a novel NF2/ERM4.1 superfamily gene, ehm2, that is expressed in high-metastatic K1735 murine melanoma cells. *Genomics* **65**, 113-120.
- Shook, D. and Keller, R. (2003). Mechanisms, mechanics and function of epithelial-mesenchymal transitions in early development. *Mech. Dev.* **120**, 1351-1383.
- Tanoue, T. and Takeichi, M. (2004). Mammalian Fat1 cadherin regulates actin dynamics and cell-cell contact. *J. Cell Biol.* **165**, 517-528.
- Wang, J., Cai, Y., Penland, R., Chauhan, S., Miesfeld, R. L. and Ittmann, M. (2006). Increased expression of the metastasis-associated gene Ehm2 in prostate cancer. *Prostate* **66**, 1641-1652.
- Wang, Q. and Margolis, B. (2007). Apical junctional complexes and cell polarity. *Kidney Int.* **72**, 1448-1458.
- Widmann, T. J. and Dahmann, C. (2009). Dpp signaling promotes the cuboidal-to-columnar shape transition of *Drosophila* wing disc epithelia by regulating Rho1. *J. Cell Sci.* **122**, 1362-1373.